BPS Dendroscopy on Local CY threefolds

Boris Pioline

Advances in String Theory and QFT
(Unofficial PiljinFest)
KIAS, 31/5/2024

Thanks to my wonderful co-authors



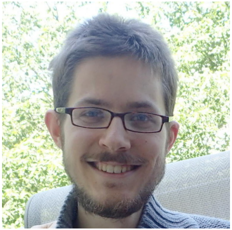


Based on 'BPS Dendroscopy on Local $\mathbb{P}^2$' [2210.10712]
with Pierrick Bousseau, Pierre Descombes and Bruno Le Floch

and 'BPS Dendroscopy on Local $\mathbb{F}_0$' with BL and Rishi Raj, to appear

δενδρον= tree

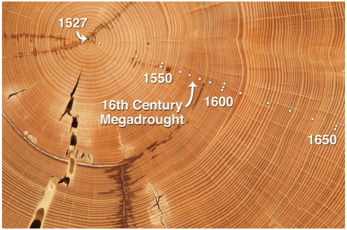

Dendrochronology

Dentrology

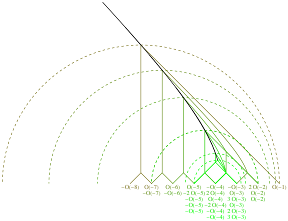

Dendroscopy

Introduction

- In type IIA string theory compactified on a Calabi-Yau threefold X, the BPS spectrum consists of bound states of D6-D4-D2-D0 branes, with charge $\gamma \in H_{\text{even}}(X, \mathbb{Q})$.
- BPS states saturate the bound $M(\gamma) \geq |Z(\gamma)|$, where the central charge $Z \in \text{Hom}(\Gamma, \mathbb{C})$ depends on the complexified Kähler moduli.
- The index $\Omega_z(\gamma)$ counting BPS states is robust under complex structure deformations, but in general depends on $z \in \mathcal{M}_K$.
- Mathematically, the Donaldson-Thomas invariant $\Omega_z(\gamma)$ counts stable objects with $\text{ch}\, E = \gamma$ in the derived category of coherent sheaves $\mathcal{C} = D^b\text{Coh}(X)$, and depend on a choice of Bridgeland stability condition $z \in \text{Stab}\, \mathcal{C} \supset \mathcal{M}_K$.

Introduction

- $\Omega_z(\gamma)$ is locally constant on $\mathrm{Stab}\,\mathcal{C}$, but can jump across real codimension one walls of marginal stability $\mathcal{W}(\gamma_L, \gamma_R) \subset \mathcal{M}_K$, where the phases of the central charges $Z(\gamma_L)$ and $Z(\gamma_R)$ become aligned *[Kontsevich Soibelman'08, Joyce Song'08]*
- Physically, multi-centered black hole solutions with charges $\gamma = m_{L,}\gamma_L + m_{R,}\gamma_R$ (dis)appear across the wall

$$r = \frac{\langle \gamma_L, \gamma_R \rangle \, |Z(\gamma_L + \gamma_R)|}{\mathrm{Im}[\bar{Z}(\gamma_L)\, Z(\gamma_R)]}$$

$$\Delta\Omega(\gamma) = \pm\, |\langle \gamma_L, \gamma_R \rangle|\, \Omega(\gamma_L)\Omega(\gamma_R)$$

Denef'02, Denef Moore '07, ...

Introduction

- Most of these bound states are expected to decay away as one follows the attractor flow equations *[Ferrara Kallosh Strominger'95]*

$$\mathrm{AF}_\gamma : \quad r^2 \frac{\mathrm{d}z^a}{\mathrm{d}r} = -g^{a\bar{b}} \partial_{\bar{b}} |Z_z(\gamma)|^2$$

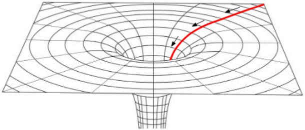

- Let $z_\star(\gamma)$ be the endpoint of the flow, or attractor point. Since $|Z_z(\gamma)|^2$ decreases along the flow, $z_\star(\gamma)$ can either be a regular local minimum of $|Z_z(\gamma)|$ with $|Z_{z_\star(\gamma)}(\gamma)| > 0$, or a conifold point on the boundary of $\mathrm{Stab}\,\mathcal{C}$ if $Z_{z_\star(\gamma)}(\gamma) = 0$.
- We define the attractor invariant as $\Omega_\star(\gamma) = \Omega_{z_\star(\gamma)}(\gamma)$.

The Split Attractor Flow Conjecture

- Starting from $z \in \mathcal{M}_K$, following AF_γ and recursively applying the WCF formula whenever the flow crosses a wall of marginal stability, one can *in principle* express $\Omega_z(\gamma)$ in terms of attractor invariants $\Omega_*(\gamma_i)$.

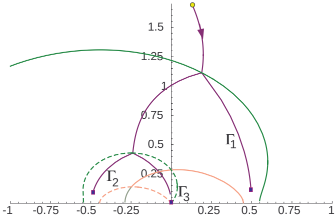

Denef Moore'07

The Split Attractor Flow Conjecture (SFAC)

- In terms of the rational DT invariants *[Joyce Song 08, Manschot BP Sen 11]*

$$\bar{\Omega}_z(\gamma) := \sum_{k|\gamma} \frac{y-1/y}{k(y^k-y^{-k})} \Omega_z(\gamma/k)_{y\to y^k} \overset{y\to 1}{\to} \sum_{k|\gamma} \frac{1}{k^2} \Omega_z(\gamma/k)$$

  the result takes the form

$$\bar{\Omega}_z(\gamma) = \sum_{\gamma=\sum \gamma_i} \frac{g_z(\{\gamma_i\}, y)}{\mathrm{Aut}(\{\gamma_i\})} \prod_i \bar{\Omega}_\star(\gamma_i)$$

  where $g_z(\{\gamma_i\}, y)$ is a sum over attractor flow trees.

- The Split Attractor Flow Conjecture is the statement that for any $z \in \mathcal{M}_K$, only a finite number of decompositions $\gamma = \sum \gamma_i$ contribute to the index $\bar{\Omega}_z(\gamma)$.

  [Denef'00, Denef Greene Raugas'01,Denef Moore'07]

The Split Attractor Flow Conjecture

- Unfortunately it is not clear a priori which constituents γ_i can contribute, except for the obvious constraints

$$\sum_i \gamma_i = \gamma \ , \quad \sum_i |Z_{z_\star(\gamma_i)}(\gamma_i)| < |Z_z(\gamma)|$$

- In particular, there can be cancellations between D-branes and anti-D-branes, and contributions from conifold states which are massless at their attractor point are difficult to bound.
- Even if SAFC holds, one still has to compute the attractor indices $\Omega_\star(\gamma)$, a tall order for compact CY3, which generally admit regular attractor points.

Simplifications for local CY3

- First, because the central charge $Z_z(\gamma)$ is holomorphic, $|Z_z(\gamma)|^2$ has no local minima so the only attractor points are conifold points with $Z_z(\gamma_i) = 0$.
- Second, the phase of $Z(\gamma)$ is conserved along the attractor flow:

$$r^2 \frac{\mathrm{d}}{\mathrm{d}r} \log \frac{Z(\gamma)}{\bar{Z}(\gamma)} = -\partial_a Z(\gamma) g^{a\bar{b}} \partial_{\bar{b}} \bar{Z}(\gamma) + \partial_a Z(\gamma) g^{a\bar{b}} \partial_{\bar{b}} \bar{Z}(\gamma) = 0$$

The BPS spectrum for fixed phase is conveniently encoded in the scattering diagram $\mathcal{D}_\psi = \cup_\gamma \mathcal{R}_\psi(\gamma)$, i.e. the union of active rays

$$\mathcal{R}_\psi(\gamma) = \{z \in \mathrm{Stab}\,\mathcal{C}, \Omega_z(\gamma) \neq 0, \arg Z(\gamma) = \psi + \tfrac{\pi}{2}\}$$

The WCF gives strong consistency conditions when rays intersect.

Simplifications for local CY3

- Third, $\mathcal{C} = D^b\,\mathrm{Coh}(X)$ is isomorphic (in many ways) to the derived category of representations $D^b\,\mathrm{Rep}(Q, W)$ of certain quivers with potential, associated to exceptional collections on X. Physically, quiver nodes correspond to fractional branes with $\Omega_\star(\gamma_i) = 1$.
- In "quiver regions" where the objects of charge γ_i are stable *and* their central charges $Z(\gamma_i)$ lie in a common half-plane, the BPS spectrum reduces to the SUSY vacua of Quiver Quantum mechanics, or mathematically to the set of semi-stable representations of (Q, W).
- Finally, one can argue that the only attractor-stable BPS bound states are those associated to the objects in the collection, i.e. $\Omega_\star(\gamma) = 0$ unless $\gamma = \gamma_i$. This determines the scattering diagram in the quiver regions, and everywhere by consistency.

Outline

- In this talk, I will apply these ideas to determine the BPS spectrum for the simplest examples of CY threefolds, namely $X = K_S$ for $S = \mathbb{P}^2$ and $S = \mathbb{F}_0 = \mathbb{P}^1 \times \mathbb{P}^1$.
- We first construct the scattering diagram in the large volume region, where the central charge is given by the classical expression $Z(\gamma) \sim -\int_S e^{-zH}\,\mathrm{ch}(E)$, quadratic in z.
- We then include corrections from worldsheet instantons and construct the scattering diagram on the physical slice of Π-stability conditions.
- The resulting diagram interpolates between the quiver and large volume scattering diagrams, and reveals the action of the group of auto-equivalences $\Gamma_1(3)$ for $S = \mathbb{P}^2$, or $\Gamma_1(4)$ for $S = \mathbb{F}_0$.

Scattering diagram for quivers

- Let (Q, W) a quiver with potential, $\gamma = (N_1, \dots, N_K) \in \mathbb{N}^{Q_0}$ a dimension vector and $\theta = (\theta_1, \dots, \theta_K) \in \mathbb{R}^{Q_0}$ a stability vector such that $(\theta, \gamma) = 0$.
- This data defines a supersymmetric quantum mechanics with 4 supercharges, gauge group $G = \prod_i U(N_i)$, superpotential W, FI parameters θ_i. SUSY Higgs vacua are harmonic forms on

$$\mathcal{M}_\theta(\gamma) = \{ \sum_{a:i\to j} |\Phi_a|^2 - \sum_{a:j\to i} |\Phi_a|^2 = \theta_i, \quad \partial_{\Phi_a} W = 0 \} / G$$

- Mathematically, $\mathcal{M}_\theta(\gamma)$ is the moduli space of θ-semi-stable representations of (Q, W) (i.e. $(\theta, \gamma') \le (\theta, \gamma)$ for any subrep) and the refined BPS index $\Omega_\theta(\gamma, y)$ is (roughly) its Poincaré polynomial.
- $\Omega_\theta(\gamma, y)$ may jump on real codimension 1 walls when the inequality is saturated (and on real codimension 2 loci when W is varied).

Scattering diagram for quivers

- The BPS indices are conveniently encoded in the scattering diagram $\mathcal{D}(Q,W)$,namely is the union of the real codimension-one rays $\{\mathcal{R}(\gamma), \gamma\in\mathbb{N}^{Q_0}\}$ with *[Bridgeland'16]*

$$\mathcal{R}(\gamma) = \{\theta\in\mathbb{R}^{Q_0} : (\theta,\gamma)=0,\ \bar\Omega_\theta(\gamma)\neq 0\}$$

- Each point along $\mathcal{R}(\gamma)$ is equipped with an automorphism of the quantum torus algebra,

$$\mathcal{U}_\theta(\gamma) = \exp\left(\frac{\bar\Omega_\theta(\gamma)}{y^{-1}-y}\mathcal{X}_\gamma\right)\ ,\quad \mathcal{X}_\gamma\mathcal{X}_{\gamma'} = (-y)^{\langle\gamma,\gamma'\rangle}\mathcal{X}_{\gamma+\gamma'}$$

- The WCF ensures that the diagram is consistent: for any generic closed path $\mathcal{P}: t\in[0,1]\to\mathbb{R}^{Q_0}$, $\prod_i \mathcal{U}_{\theta(t_i)}(\gamma_i)^{\epsilon_i}=1$

Scattering diagram for Kronecker quiver

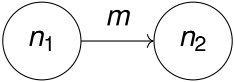

$$\theta_1 > 0, \theta_2 < 0 : \quad \dim \mathcal{M}_\theta(\gamma) = m n_1 n_2 - n_1^2 - n_2^2 + 1$$

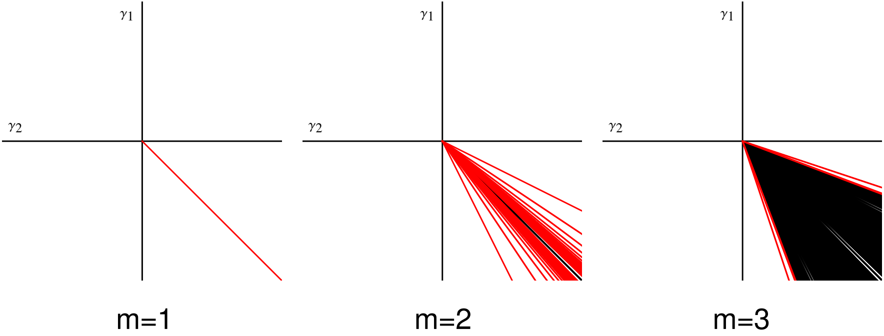

Attractor invariants for quivers

- The analogue of the attractor point for quivers is the self-stability condition *[Manschot BP Sen'13; Bridgeland'16]*

$$(\theta_\star(\gamma), \gamma') = \langle \gamma', \gamma \rangle := \sum_{a:i \to j} (n'_i n_j - n'_j n_i)$$

Let $\Omega_\star(\gamma) := \Omega_{\theta_\star(\gamma)}(\gamma)$ be the attractor invariant.

- Easy fact: for quivers without oriented loops, the only non-vanishing attractor invariants are supported on basis vectors associated to simple representations, $\Omega_\star(\gamma_i) = 1$.
- The consistency of $\mathcal{D}(Q, W)$ uniquely determines all rays in terms of the initial rays $\mathcal{R}_\star(\gamma)$, defined as those which contain $\theta_\star(\gamma)$.
- The Flow Tree Formula of *[Alexandrov BP'18]* determines the indices of outgoing rays produced by scattering initial rays *[Argüz Bousseau '20]*.

Quivers for local CY3

- Whenever a CY threefold X admits a (strong, full, cyclic) exceptional collection E, the category $D^b \operatorname{Coh} X$ is isomorphic to the category $D^b \operatorname{Rep}(Q, W)$ of representations of the quiver with potential associated to E. *[Bondal'90]*
- When X is toric, there is a simple prescription to obtain (Q, W) from brane tilings/periodic quivers. Eg. for $X = K_{\mathbb{P}^2}$,

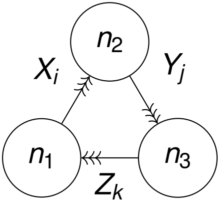

$$W = \sum \epsilon_{ijk} X_i Y_j Z_k$$

$$\begin{aligned} \gamma_1 &= [-1, 0, 0] \\ \gamma_2 &= [2, -1, -\tfrac{1}{2}] \\ \gamma_3 &= [-1, 1, -\tfrac{1}{2}] \end{aligned}$$

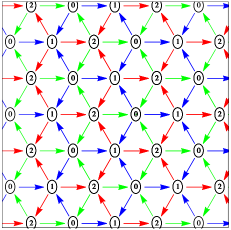

Attractor invariants for $K_{\mathbb{P}^2}$

- By studying expected dimension of the moduli space of semi-stable representations $\mathcal{M}_\theta(\gamma)$, *[Beaujard BP Manschot'20]* conjectured that the attractor index $\Omega_\star(\gamma)$ vanishes unless $\gamma = \gamma_i$ or γ lies in the kernel of the Dirac pairing.
- For toric local del Pezzo surfaces, this conjecture was tested and refined by *[Mozgovoy BP '20]* and *[Descombes'21]*: $\Omega_\star(\gamma) = 0$ unless $\gamma = \gamma_i$ or $\gamma = k[D0]$, with $\Omega(k[D0]) = -y^3 - b_2 y - 1/y$. This is now a theorem for $X = K_{\mathbb{P}^2}$ *[Bousseau Descombes Le Floch BP'22]*.
- This allows to construct the quiver scattering diagram inductively, and describe any BPS state in terms of attractor flow trees.

Quiver scattering diagram for $K_{\mathbb{P}^2}$

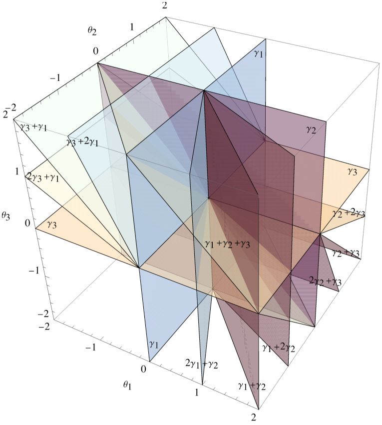

A 2D slice of the orbifold scattering diagram

Let $\mathcal{D}_o$ be the restriction of $\mathcal{D}(Q, W)$ to the hyperplane $\theta_1 + \theta_2 + \theta_3 = 1$:

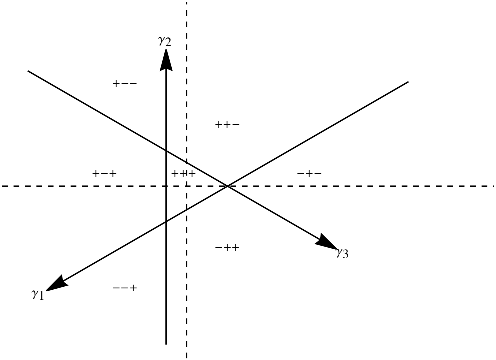

A 2D slice of the orbifold scattering diagram

Let $\mathcal{D}_o$ be the restriction of $\mathcal{D}(Q, W)$ to the hyperplane $\theta_1 + \theta_2 + \theta_3 = 1$:

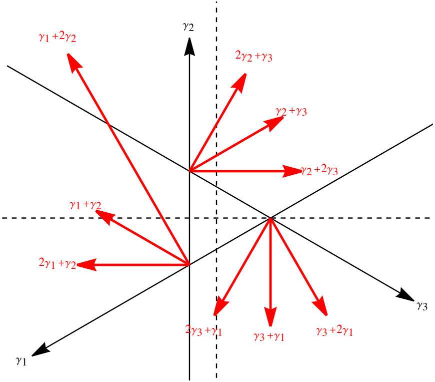

Let $\mathcal{D}_o$ be the restriction of $\mathcal{D}(Q, W)$ to the hyperplane $\theta_1 + \theta_2 + \theta_3 = 1$:

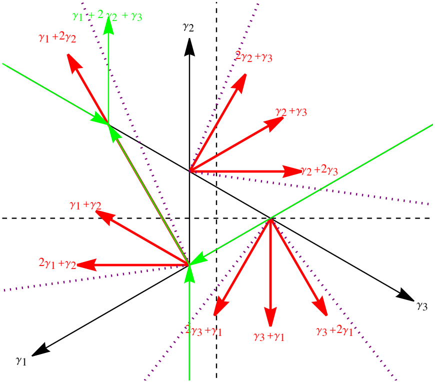

A 2D slice of the orbifold scattering diagram

The full scattering diagram $\mathcal{D}_o$ includes regions with dense set of rays:

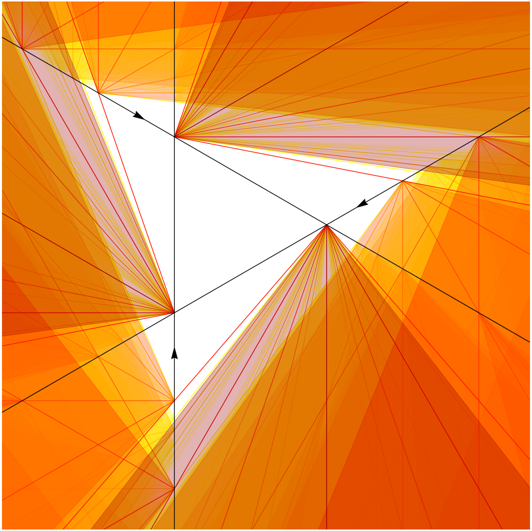

Bridgeland stability conditions

- More generally, Donaldson-Thomas invariants are defined in Bridgeland's framework of stability conditions on a triangulated CY3 category $\mathcal{C}$.
- A stability condition is a pair $\sigma = (Z, \mathcal{A})$ where $Z : \Gamma \to \mathbb{C}$ is a linear map and $\mathcal{A} \subset \mathcal{C}$ an Abelian subcategory (heart of t-structure) satisfying various axioms, e.g. $\mathrm{Im} Z(\gamma(E)) \geq 0 \ \forall E \in \mathcal{A}$.
- When it is not empty, the space $\mathrm{Stab}\,\mathcal{C}$ is a complex manifold of dimension $d = \dim K(\mathcal{C}) = \dim H^{\rm even}_{cpt}(X)$. For $X = K_S$, $d = 1 + b_2(S) + 1$.
- The group $\widetilde{GL(2,\mathbb{R})}^+$ acts on $\mathrm{Stab}\,\mathcal{C}$ by linear transformations of $(\mathrm{Re} Z, \mathrm{Im} Z)$ with positive determinant, leaving $\Omega_\sigma(\gamma)$ invariant. This effectively reduces $d \mapsto d - 2 = b_2(S)$.

Scattering diagrams on triangulated categories

- For a general triangulated category $\mathcal{C}$, define the scattering diagram $\mathcal{D}_\psi(\mathcal{C})$ as the union of codimension-one loci in $\mathrm{Stab}\,\mathcal{C}$,

$$\mathcal{R}_\psi(\gamma) = \{\sigma : \arg Z(\gamma) = \psi + \tfrac{\pi}{2},\ \bar\Omega_Z(\gamma) \neq 0\}$$

equipped with the (suitably regularized) automorphism

$$\mathcal{U}_\sigma(\gamma) = \exp\left(\frac{\bar\Omega_\sigma(\gamma)}{y^{-1}-y}\mathcal{X}_\gamma\right) = \mathrm{Exp}\left(\frac{\Omega_\sigma(\gamma)}{y^{-1}-y}\mathcal{X}_\gamma\right)$$

- The WCF ensures that the diagram $\mathcal{D}_\psi(\mathcal{C})$ is still locally consistent at each codimension-two intersection.
- A quiver description (Q, W) is valid whenever i) the simple objects in the exceptional collection are stable and ii) their central charges $Z(\gamma_i)$ lie in a common half-plane. In this region, $\mathcal{D}_\psi(\mathcal{C})$ must reduce to $\mathcal{D}(Q, W)$ upon setting $\theta_i = -\mathrm{Re}(e^{-\mathrm{i}\psi} Z(\gamma_i))$.

Large volume scattering diagram

- Consider the large volume slice with

$$Z^{\rm LV}(\gamma) = -rT_D + dT - {\rm ch}_2, \quad T_D = \frac{1}{2}T^2, \quad T = s + {\rm i}t$$

- Since $\mathrm{Re}Z(\gamma) = \frac{1}{2}r(t^2 - s^2) + ds - {\rm ch}_2$ that each ray $\mathcal{R}_0(\gamma)$ is contained in a branch of hyperbola asymptoting to $t = \pm(s - \frac{d}{r})$ for $r \neq 0$, or a vertical line when $r = 0$. Walls of marginal stability $\mathcal{W}(\gamma, \gamma')$ are half-circles centered on real axis.

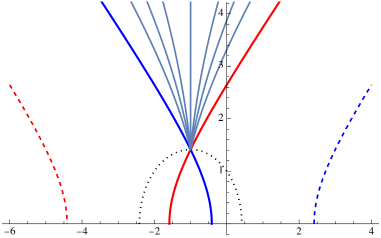

Large volume scattering diagram

- The objects $\mathcal{O}(m)$ and $\mathcal{O}(m)[1]$ are known to be stable throughout the large volume slice *[Arcara Bertram (2013)]*. The corresponding rays are 45 degree lines ending at $s = m$.
- The region of validity of the orbifold exceptional collection and its mutations are valid covers the vicinity of the boundary at $t = 0$, hence there can be no other initial ray. *[Bousseau'19]*.

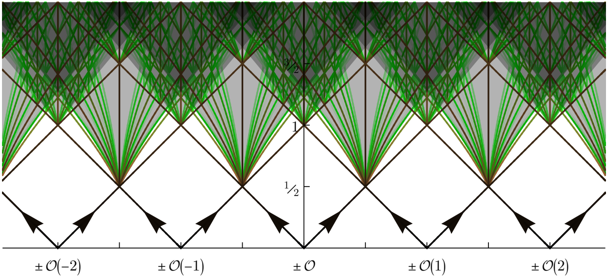

Scattering diagram in affine coordinates

Actually, Bousseau used different coordinates such that the rays become line segment $rx + dy - \mathrm{ch}_2 = 0$. This works for any ψ:

$$x = \frac{\mathrm{Re}\left(e^{-\mathrm{i}\psi} T\right)}{\cos\psi}\ , \quad y = -\frac{\mathrm{Re}\left(e^{-\mathrm{i}\psi} T_D\right)}{\cos\psi} > -\frac{1}{2}x^2$$

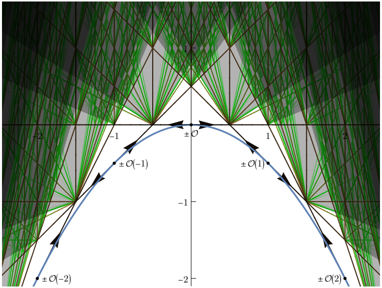

Flow tree formula at large radius

- This implies that all BPS states at large volume must arise as bound states of fluxed D4 and anti D4-branes. But how to find the possible constituents for given γ and (s, t) ?
- Think of $\mathcal{R}(\gamma)$ as the worldline of a fictitious particle of charge r, mass $M^2 = \frac{1}{2}d^2 - r\,\mathrm{ch}_2$ moving in a constant electric field. This makes it clear that constituents must lie in the past light cone.
- Moreover, the 'electric potential' $\varphi_s(\gamma) = 2(d - sr) = 2\mathrm{Im}Z_\gamma/t$ increases along the flow. The first scatterings occur after a time $t \geq \frac{1}{2}$, after each constituent $k_i\mathcal{O}(m_i)$ has moved by $|\Delta s| \geq \frac{1}{2}$, by which time $\varphi_s(\gamma_i) \geq |k_i|$.
- Since $\varphi_s(\gamma)$ is additive at each vertex, this gives a bound on the number and charges of constituents contributing to $\Omega_{(s,t)}(\gamma)$:

$$\sum_i k_i[1, m_i, \frac{1}{2}m_i^2] = \gamma \ , \quad s - t \leq m_i \leq s + t, \quad \sum |k_i| \leq \varphi_s(\gamma)$$

Thus, SAFC holds along the large volume slice !

Flow trees for $\gamma = [0, 4, 1)$

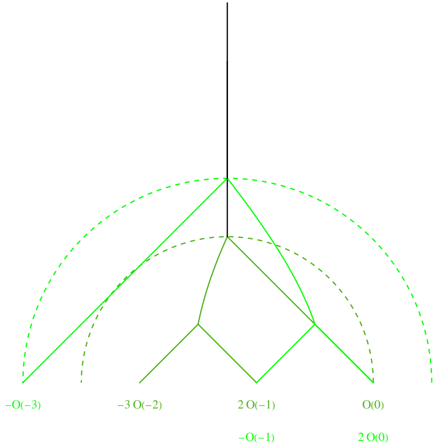

- $\{\{-3\mathcal{O}(-2), 2\mathcal{O}(-1)\}, \mathcal{O}\}$:
  $K_3(2,3)K_{12}(1,1) \to -156$
- $\{-\mathcal{O}(-3), \{-\mathcal{O}(-1), 2\mathcal{O}\}\}$:
  $K_3(1,2)K_{12}(1,1) \to -36$

Total: $\Omega_\infty(\gamma) = -192 = GV_4^{(0)}$

Flow trees for $\gamma = [1, 0, -3)$

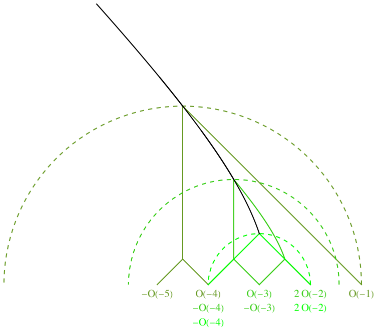

- $\{\{-\mathcal{O}(-5), \mathcal{O}(-4)\}, \mathcal{O}(-1)\}$
  $K_3(1,1)^2 \to 9$
- $\{\{-\mathcal{O}(-4), \mathcal{O}(-3)\},$
  $\{-\mathcal{O}(-3), 2\mathcal{O}(-2)\}\}$
  $K_3(1,1)^2 K_3(1,2) \to 27$
- $\{-\mathcal{O}(-4), 2\mathcal{O}(-2)\}$
  $K_6(1,2) \to 15$

Total: $\Omega_\infty(\gamma) = 51 = \chi(\mathrm{Hilb}_4 \mathbb{P}^2)$

Large volume scattering diagram for local $\mathbb{F}_0$

- For $S = \mathbb{F}_0 = \mathbb{P}^1 \times \mathbb{P}^1$, the space of Bridgeland stability conditions (modulo $GL(2,\mathbb{R})^+$) is parametrized by the Kähler moduli T_1, T_2. We focus on the canonical polarization where $\mathrm{Im}\, T_1 = \mathrm{Im}\, T_2$, and set $T_1 = T = x + \mathrm{i}t$, $T_2 = T + m$ with m real.
- The large volume slice is given by

$$Z^{\mathrm{LV}}(\gamma) = -rT(T+m) + d_1 T + d_2(T+m) - \mathrm{ch}_2$$

  The geometric rays are similar as for local $\mathbb{P}^2$, with $[r, d, \mathrm{ch}_2]$ replaced by $[2r, d_1 + d_2 - mr, \mathrm{ch}_2 - md_2]$. Set $\psi = 0$ for simplicity.
- The objects $\mathcal{O}(d_1, d_2)$, $\mathcal{O}(d_1, d_2)[1]$ are stable throughout the large volume slice *[Arcara Miles'14]*. The ray $\mathcal{R}_0(\mathcal{O}(d_1, d_2)$ starts at $x = \min(d_1 - m, d_2)$ and bends to the left. Similarly, $\mathcal{R}_0(\mathcal{O}(d_1, d_2)[1]$ starts at $x = \max(d_1 - m, d_2)$ and bends right.

Large volume scattering diagram for local $\mathbb{F}_0$

- The category $D^b\,\mathrm{Coh}\,X$ is isomorphic to the derived category of representations for the quiver (or one of its mutations)

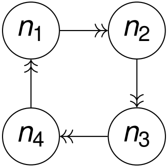

$$W = \sum_{\substack{(\alpha\beta)\in S_2\\(\gamma\delta)\in S_2}} \mathrm{sgn}(\alpha\beta)\,\mathrm{sgn}(\gamma\delta)\,\Phi_{12}^{\alpha}\,\Phi_{23}^{\gamma}\,\Phi_{34}^{\beta}\,\Phi_{41}^{\delta}$$

$$\begin{aligned}\gamma_1 &= [1,0,0,0]\\ \gamma_2 &= [-1,1,0,0]\\ \gamma_3 &= [-1,-1,1,1]\\ \gamma_4 &= [1,0,-1,0]\end{aligned}$$

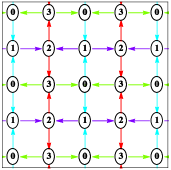

- The validity of the (mutated, shifted) quiver near $t=0$ allows to rule out other initial rays beyond $\mathcal{O}(d_1,d_2)$ and $\mathcal{O}(d_1,d_2)[1]$.

Le Floch BP Raj, to appear

Initial rays for local $\mathbb{F}_0$ at large volume, $m = 1/2$

In (x, t) coordinates, $\psi = 0$:

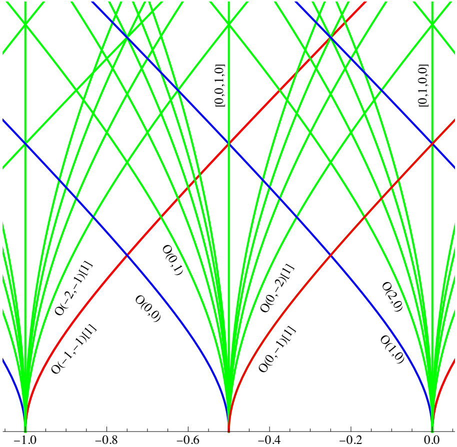

Initial rays for local $\mathbb{F}_0$ at large volume, $m = 1/2$

In (x, y) coordinates, $\psi = 0$:

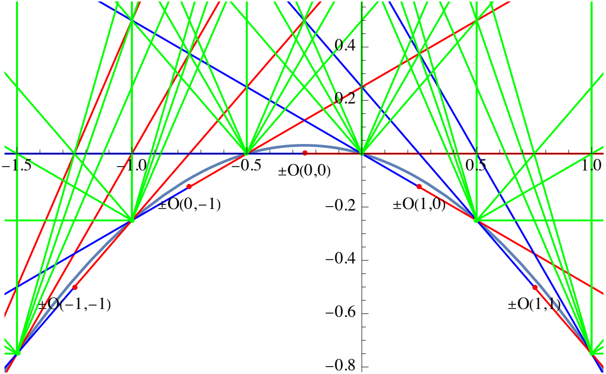

The infinite sets of rays originating from $x \in \mathbb{Z}$ and $x = \mathbb{Z} - m$ come from the scattering of two rays $\mathcal{R}(\gamma_1), \mathcal{R}(\gamma_2)$ with $\langle \gamma_1, \gamma_2 \rangle = 2$ below the parabola !

Kähler moduli space

- Mirror symmetry selects a particular Lagrangian subspace $\Pi \subset \mathsf{Stab}\,\mathcal{C}$ in the space of Bridgeland stability conditions.
- For local del Pezzo surfaces, the mirror CY3 is (a conic bundle over) a genus one curve Σ. (T_i, T_D) are given by periods of a holomorphic differential with logarithmic singularities, and satisfy Picard-Fuchs equations.
- Rather than working with flat coordinates T_i, it is advantageous to use (τ, m_i) where τ parametrizes the Coulomb branch while m_i are mass parameters in the 5D gauge theory.
- Near the large volume point, mirror symmetry ensures that $Z_\tau(\gamma) \sim -\int_S e^{-\tau H} \sqrt{\mathrm{Td}(S)}\,\mathrm{ch}(E)$, up to worldsheet instantons. Using $GL(2,\mathbb{R})^+$, one can absorb the corrections and use the simpler form $Z_\tau(\gamma) = -\int_S e^{-\tau H}\,\mathrm{ch}(E)$.

Modularity in Kähler moduli space

- In some cases, the monodromy group is a subgroup $\Gamma \subset SL(2,\mathbb{Z})$, and the universal cover of $\mathcal{M}_K = \mathbb{H}/\Gamma$ becomes the Poincaré half-plane $\mathbb{H}$. *[Closset Magureanu 2021; Aspman Fürrer Manschot 2021]*
- This happens for $X = K_{\mathbb{P}^2}$, where $\Gamma = \Gamma_1(3)$, and for $X = K_{\mathbb{F}_0}$ at special points $m \in \mathbb{Z}$ where $\Gamma = \Gamma_0(8)$. For generic m, $\Gamma = \Gamma_1(4)$ with a square root branch cut.

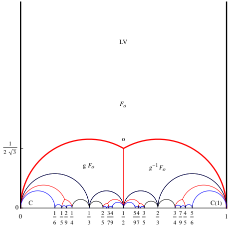

$K_{\mathbb{P}^2}$: $\Gamma_1(3)$

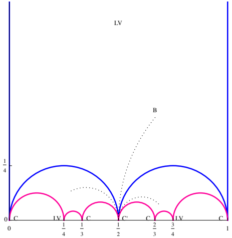

$K_{\mathbb{F}_0}$: $\Gamma_1(4)$

Central charge as Eichler integral

- It turns out that $\partial_\tau \lambda$ is holomorphic, so its periods are proportional to $(1,\tau)$. Integrating along a path from reference point o to τ, one finds an Eichler integral representation

$$\boxed{\begin{pmatrix} T \\ T_D \end{pmatrix} = \begin{pmatrix} T^o \\ T^o_d \end{pmatrix} + \int_{\tau_o}^{\tau} \begin{pmatrix} 1 \\ u \end{pmatrix} C(u)\,\mathrm{d}u}$$

where $C(\tau)$ is a weight 3 modular form:

$$C_{\mathbb{P}^2} = \frac{\eta(\tau)^9}{\eta(3\tau)^3}, \quad C_{\mathbb{F}_0} = \frac{\eta(\tau)^4 \eta(2\tau)^6}{\eta(4\tau)^4} \sqrt{\frac{J_4+8}{J_4+8\cos\pi m}}$$

Here $J_4(\tau) = 8 + \left(\frac{\eta(\tau)}{\eta(4\tau)}\right)^8$ is the Hauptmodul for $\Gamma_1(4)$.

Central charge as Eichler integral

- This provides an computationally efficient analytic continuation of Z_τ throughout $\mathbb{H}$, and gives access to monodromies:

$$\tau \mapsto \frac{a\tau+b}{c\tau+d} \quad \begin{pmatrix} 1 \\ T \\ T_D \end{pmatrix} \mapsto \begin{pmatrix} 1 & 0 & 0 \\ m & d & c \\ m_D & b & a \end{pmatrix} \cdot \begin{pmatrix} 1 \\ T \\ T_D \end{pmatrix}$$

  where (m, m_D) are period integrals of C from τ_o to $\frac{d\tau_o-b}{a-c\tau_o}$.
- At large volume $\tau \to \mathrm{i}\infty$, using $C = 1 + \mathcal{O}(q)$ one finds

$$T = \tau + \mathcal{O}(q), \quad T_D = \frac{1}{2}\tau^2 + \frac{1}{8} + \mathcal{O}(q)$$

  in agreement with $Z_\tau(\gamma) \sim -\int_S e^{-\tau H}\sqrt{\mathrm{Td}(S)}\,\mathrm{ch}(E)$.

Exact scattering diagram for $K_{\mathbb{P}^2}$

- The scattering diagram $\mathcal{D}^{\Pi}_{\psi}$ along the physical slice should interpolate between $\mathcal{D}^{\rm LV}_{\psi}$ around $\tau = \mathrm{i}\infty$ and $\mathcal{D}_o$ around $\tau = \tau_o$, and be invariant under the action of $\Gamma_1(3)$.
- Under $\tau \mapsto \frac{\tau}{3n\tau+1}$ with $n \in \mathbb{Z}$, $\mathcal{O} \mapsto \mathcal{O}[n]$. Hence there is a doubly infinite family of initial rays emitted at $\tau = 0$, associated to $\mathcal{O}[n]$.

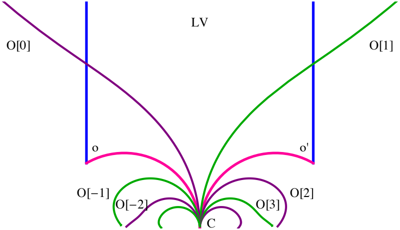

- Similarly, there must be an infinite family of initial rays coming from $\tau = \frac{p}{q}$ with $q \neq 0 \mod 3$, corresponding to $\Gamma_1(3)$-images of $\mathcal{O}$, where an object denoted by $\mathcal{O}_{p/q}$ becomes massless.

Exact scattering diagram for small ψ

- For $|\psi|$ small enough, the only rays which reach the large volume region are those associated to $\mathcal{O}(m)$ and $\mathcal{O}(m)[1]$. Thus, the scattering diagram $\mathcal{D}^{\Pi}_{\psi}$ is isomorphic to $\mathcal{D}^{\rm LV}_{0}$ inside $\mathcal{F}$ and its translates:

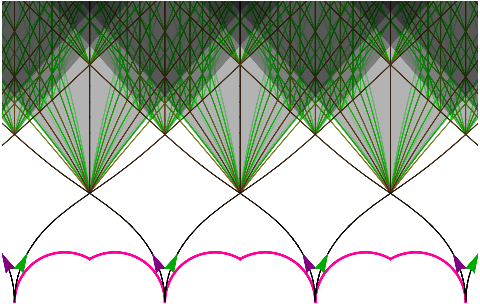

Scattering diagram in affine coordinates

- In affine coordinates, the initial rays $\mathcal{R}_{\mathcal{O}(m)}$ are still tangent to the parabola $y = -\frac{1}{2}x^2$ at $x = m$, but the origin of each ray is shifted to $x = m + \mathcal{V}\tan\psi$ where $\mathcal{V}$ is the quantum volume

$$\mathcal{V} = \mathrm{Im}\, T(0) = \frac{27}{4\pi^2}\mathrm{Im}\left[\mathrm{Li}_2(e^{2\pi \mathrm{i}/3})\right] \simeq 0.463$$

- The topology of $\mathcal{D}_\psi^\Pi$ jumps at a discrete set of rational values

$$\mathcal{V}\tan\psi \in \{\tfrac{F_{2k}+F_{2k+2}}{2F_{2k+1}}, k \geq 0\} = \{\tfrac{1}{2}, 1, \tfrac{11}{10}, \tfrac{29}{26}, \tfrac{19}{17}, \dots\}$$

and a dense set of values in $[\frac{\sqrt{5}}{2}, +\infty)$ where secondary rays pass through a conifold point.

Affine scattering diagram, $|\mathcal{V} \tan\psi| < 1/2$

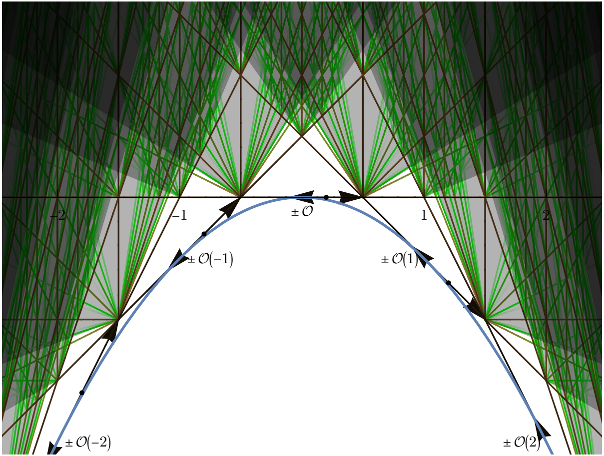

Exact scattering diagram, $\psi = 0$

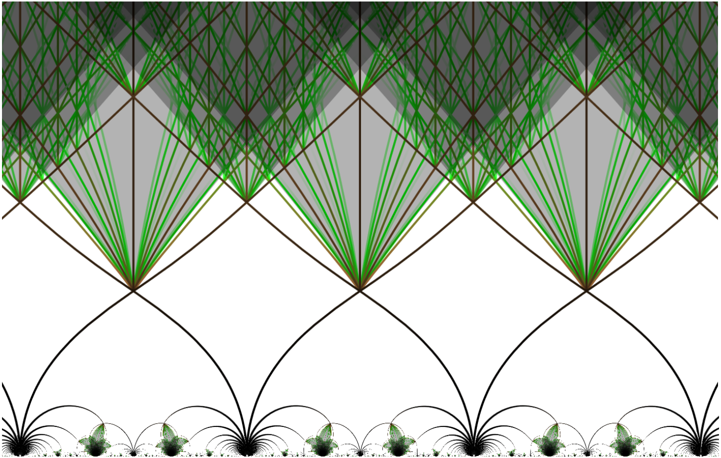

Exact scattering diagram, $\psi = 0.3$

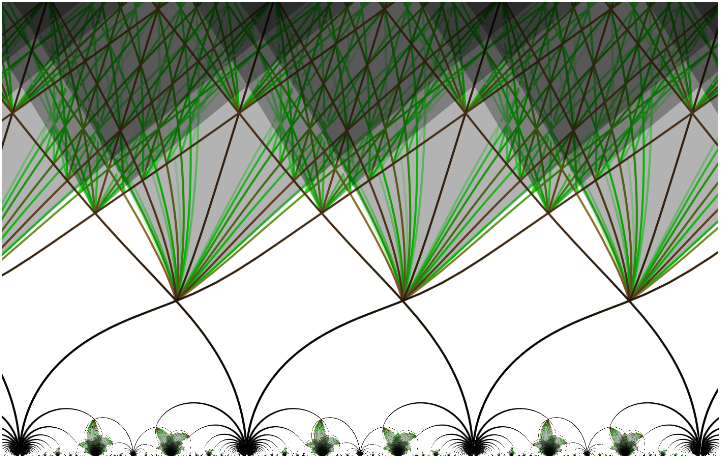

Exact scattering diagram, $\psi = 0.6$

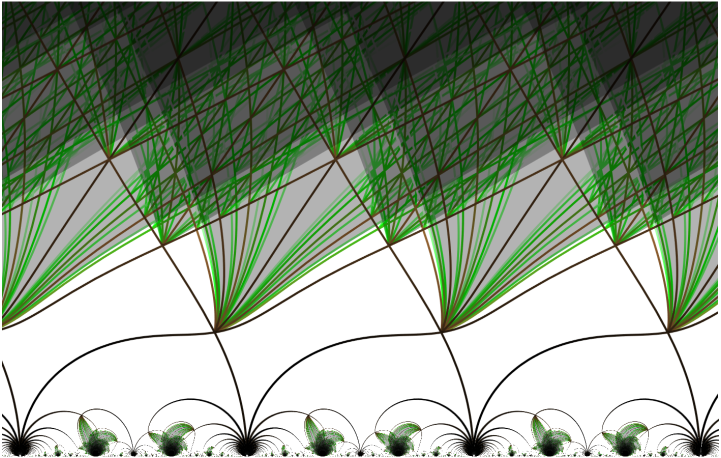

Exact scattering diagram, $\psi = 0.8$

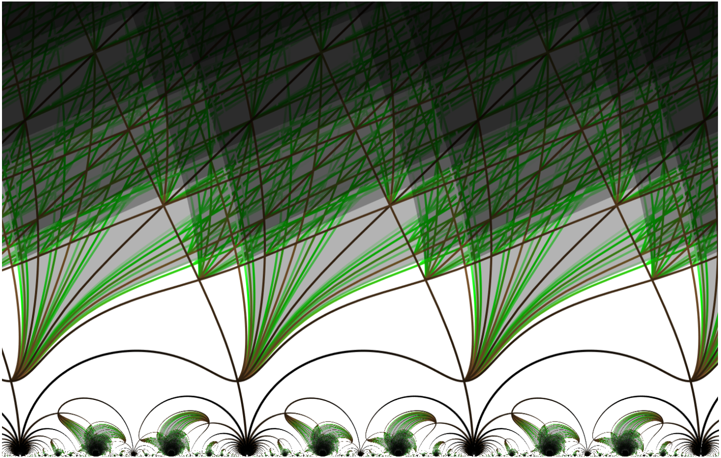

Exact scattering diagram, $\psi = 0.824$

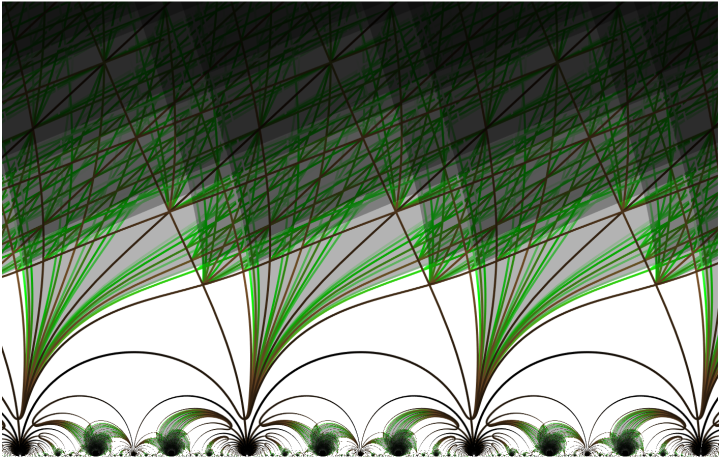

Exact scattering diagram, $\psi = 0.825$

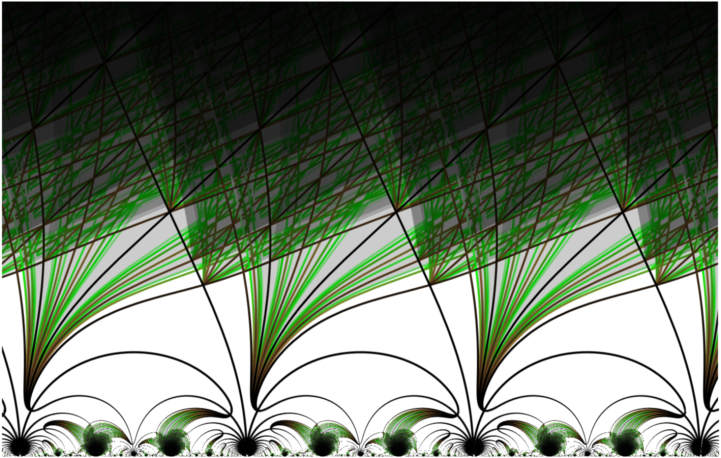

Exact scattering diagram, $\psi = 0.9$

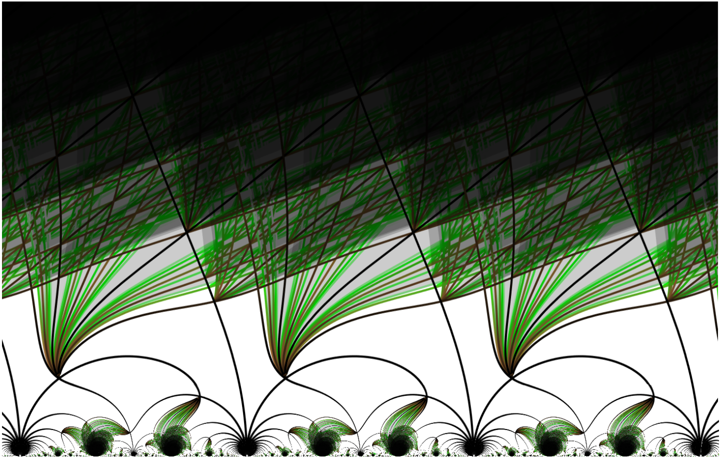

Exact scattering diagram, $\psi = 1$

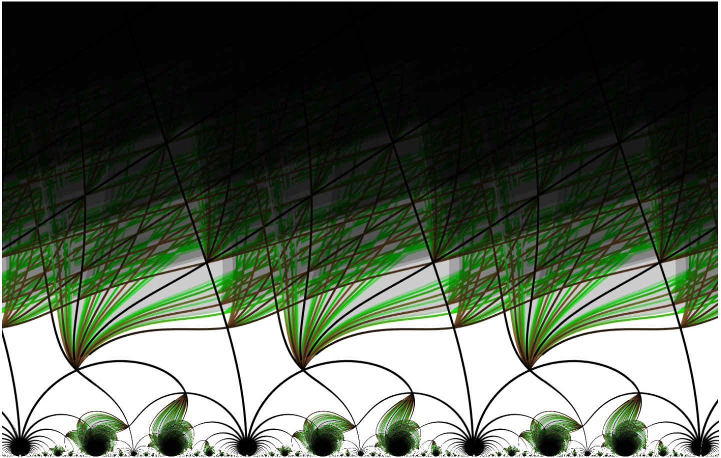

Exact scattering diagram, $\psi = 1.137$

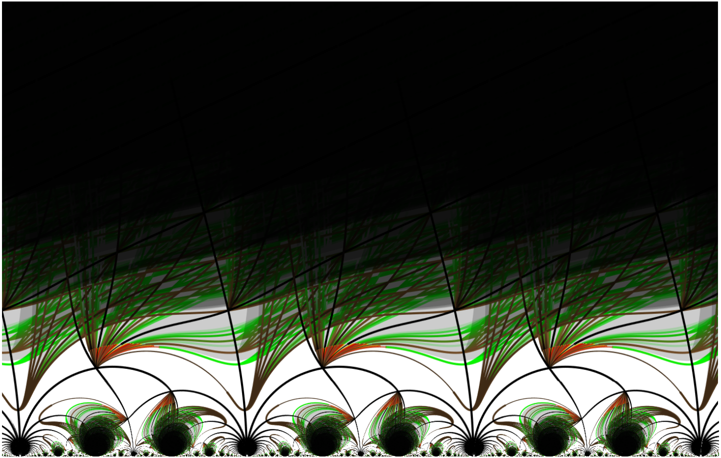

Exact scattering diagram, $\psi = 1.139$

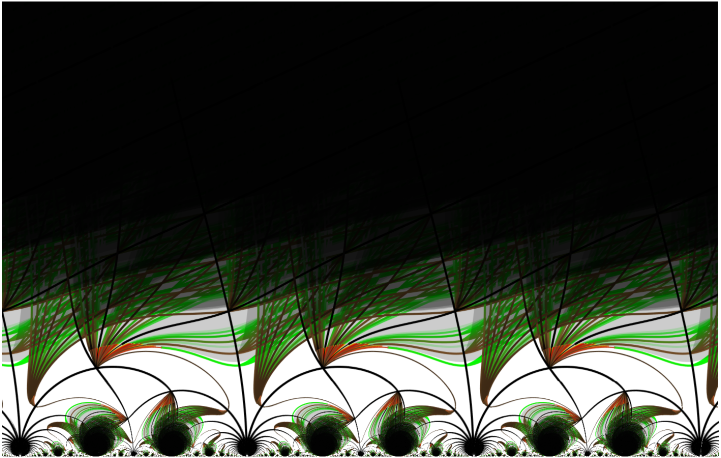

Exact scattering diagram, $\psi = \pi/2$

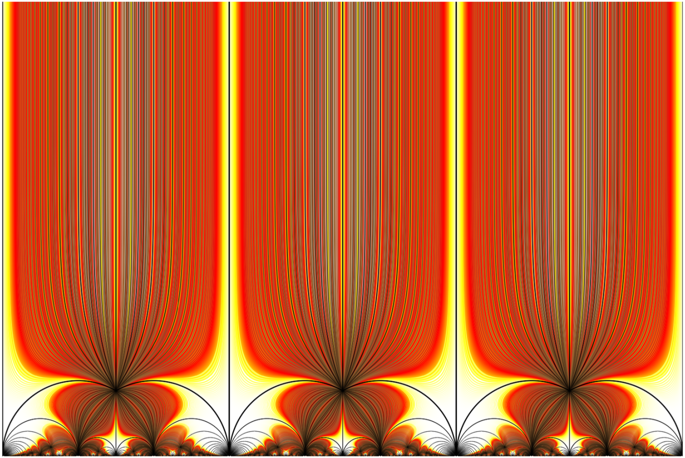

Exact scattering diagram for $\psi = \pm\frac{\pi}{2}$

- For $\psi = \pm\frac{\pi}{2}$, the geometric rays $\{\mathrm{Im} Z_\tau(\gamma) = 0\}$ coincide with lines of constant $s = \frac{\mathrm{Im}\, T_D}{\mathrm{Im}\, T} = \frac{d}{r}$, independent of ch_2:

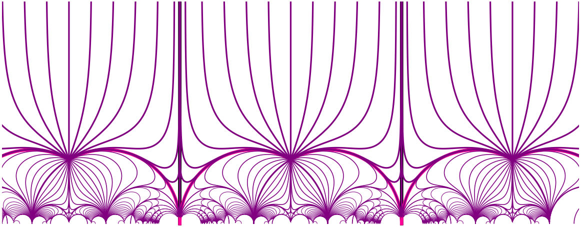

- Hence, there is no wall-crossing between τ_o and $\tau = \mathrm{i}\infty$ when $-1 \leq \frac{d}{r} \leq 0$, explaining why the Gieseker index $\Omega_\infty(\gamma)$ agrees with the quiver index $\Omega_c(\gamma)$ in the anti-attractor chamber.

Douglas Fiol Romelsberger'00, Beaujard BP Manschot'20

Fake walls and bound state metamorphosis

$\gamma = [0,1,1) = \mathrm{ch}\,\mathcal{O}_C$: $\Omega_{t\gg 1} = K_3(1,2)K_3(1,3)^{n-1} = y^2 + 1 + 1/y^2$

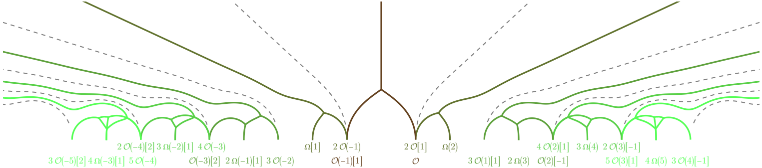

$\gamma = [1,0,1) = \mathrm{ch}\,\mathcal{O}$: $\Omega_{t\gg 1} = K_3(1,3)\dots K_3(1,3n) = 1$

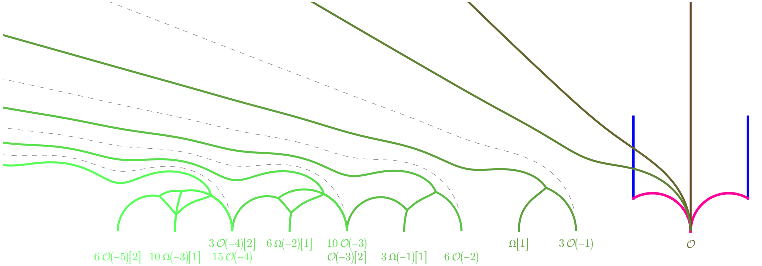

Exact scattering diagram for $K_{\mathbb{F}_0}$

- For local $\mathbb{F}_0$, the scattering diagram is complicated by branch cuts and m-dependence. The quantum volume is now

$$\mathcal{V}(m) = \frac{T(0)}{\mathrm{i}} = \frac{2\mathrm{i}}{\pi^2}\left(\mathrm{Li}_2(-\mathrm{i}e^{\mathrm{i}\pi m/2}) - \mathrm{Li}_2(\mathrm{i}e^{\mathrm{i}\pi m/2})\right)$$

  In (x, y) coordinates, the origin of the initial rays is shifted by $\Delta x = \tan\psi\,\mathrm{Re}\mathcal{V}(m) - \mathrm{Im}\mathcal{V}(m)$.

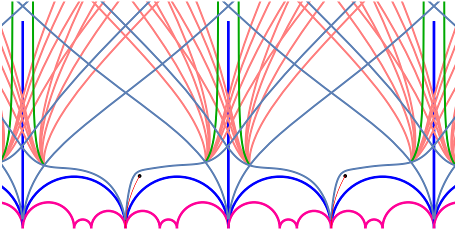

Conclusion - outlook

- Scattering diagrams provide an efficient way to organize the BPS spectrum, on local CY3 manifolds, and a natural decomposition into elementary constituents.
- It would be interesting to extend this description to other toric CY3, such as higher del Pezzo surfaces. *Caution: for $\mathbb{F}_1$, or whenever there exists curves with negative self-intersection, the fluxed D4-branes are no longer absolutely stable !*
- Attractor indices for local CY3 are very simple, how about single-centered/pure-Higgs indices ?
- For compact CY3, $Z(\gamma) = e^{K/2} Z_{\rm hol}(\gamma)$ is not longer holomorphic, so $\arg Z(\gamma)$ is not constant along the flow, and there can be initial rays not related to conifold states. Can one nonetheless use scattering diagrams to organize the BPS spectrum ?

Happy birthday Piljin !

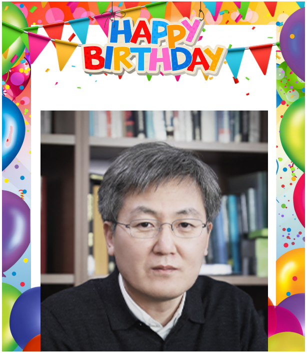

©The Happiness Foundation